





# Identification and analysis of bottom simulating reflectors in the Foz do Amazonas Basin, Northern Brazil

Laisa da Fonseca Aguiar<sup>1</sup> , Antonio Fernando Menezes Freire<sup>1\*</sup> , Cleverson Guizan Silva<sup>1</sup> ,  
Wagner Moreira Lupinacci<sup>1</sup> 

## Abstract

This work proposed an additional approach to investigate gas hydrate occurrences in the Foz do Amazonas Basin, in the Brazilian Equatorial Margin. The automatic comparison of seafloor seismic amplitudes with those from the Bottom Simulating Reflectors (BSR) was used to exhibit the reversal of signal polarities among the seafloor (positive) and the BSR (negative), reinforcing the identification of BSR in areas where its visualization was unclear. Additionally, we used the envelope attribute to highlight the BSR in the seismic section. Subsequently, we decomposed the seismic data into different frequency bands, applied a -90 degrees phase rotation to the data and recalculated the envelope attribute for each section decomposed in frequency bands. This technique improved visualization, allowing the identification of intervals where BSR were laterally discontinuous, revealing to be valuable for mapping the gas hydrate distribution in Foz do Amazonas Basin.

**KEYWORDS:** gas hydrates; Foz do Amazonas Basin; envelope attribute; seismic amplitudes; spectral decomposition.

## INTRODUCTION

The Foz do Amazonas Basin occupies a region of roughly 268,000 km<sup>2</sup>, from the coastline, across the continental shelf, slope, and the Amazon river submarine fan (Fig. 1), which is considered a large deep-sea fan (Damuth and Kumar 1975, Brandão and Feijó 1994, Figueiredo *et al.* 2007, Araújo *et al.* 2009).

The accumulation of gas hydrates in the Amazon fan was indirectly registered by the presence of Bottom Simulating Reflectors (BSR) (Manley and Flood 1988, Sad *et al.* 1998, Tanaka *et al.* 2003, Berryman *et al.* 2015). Recently, gas hydrate occurrences were confirmed in the submarine fan by Ketzer *et al.* (2018), after direct core sampling and compositional analysis of seafloor fluid seepages (Ketzer *et al.* 2018).

A BSR occurs as a seismic reflector that is usually parallel to the seafloor, coinciding with the Base of the Gas Hydrate Stability Zone (BGHSZ). These reflectors present a reversed polarity in comparison to the seafloor (Hyndman and Spence 1992, Kvenvolden 1993, 1998, Freire *et al.* 2011). The BSR corresponds to the phase boundary indicating the acoustic impedance contrast between higher compressional velocity, hydrate cemented sediment above the GHSZ, and lower compressional velocity below the GHSZ, containing free gas

(Kvenvolden 1993). Therefore, recognizing BSR can assist in mapping the distribution of natural gas hydrates (Joshi *et al.* 2017).

The BSR is an indication of the existence of gas hydrates, but does not exclude the possibility of the occurrence of gas hydrates in areas without the BSR or the presence of BSR in areas without gas hydrates (Holbrooke *et al.* 1996, Ginsburg and Soloviev 1997, Satyavani *et al.* 2008). This justifies the procedures taken in the present work to better characterize the seismic nature of the BSR in the Foz do Amazonas Basin, where gas hydrates were sampled (Ketzer *et al.* 2018).

Understanding the presence of gas hydrates on continental margins is of great importance due to its energy potential (Kvenvolden 1993, Sloan Jr. 2003, Demirbas 2010, Joshi *et al.* 2017). In addition, methane hydrates could influence the global climate due to the release of gas methane into the atmosphere, and also from the perspective of seafloor instability and as a marine geohazard (Kvenvolden 1993, Demirbas 2010, Majumdar *et al.* 2016). Another relevant aspect of studying methane hydrates is related to their promising potential in the fields of gas storage and transportation for natural gas (Di Profio *et al.* 2017). The Foz do Amazonas basin has been the focus of the investigation of gas hydrates recently, although their distribution is still poorly understood.

Seismic attributes are notably useful for seismic interpretation, presenting an increasing worth for the exploration industry (Taner *et al.* 1994). Their use enables the understanding of geological information such as physical parameters and subsurface geometry (Taner *et al.* 1979). The selection of an attribute relies on the substrate parameters, the mathematical source of the attribute, and its sensibility (Chen and Sidney 1997). Spectral decomposition is a technique that has been

<sup>1</sup>Exploratory Interpretation and Reservoir Characterization Group, Department of Geology and Geophysics, Universidade Federal Fluminense – Niterói (RJ), Brazil. E-mails: laisafonseca@id.uff.br, fernando\_freire@id.uff.br, wagnerlupinacci@id.uff.br, cguizan@id.uff.br

\*Corresponding author.



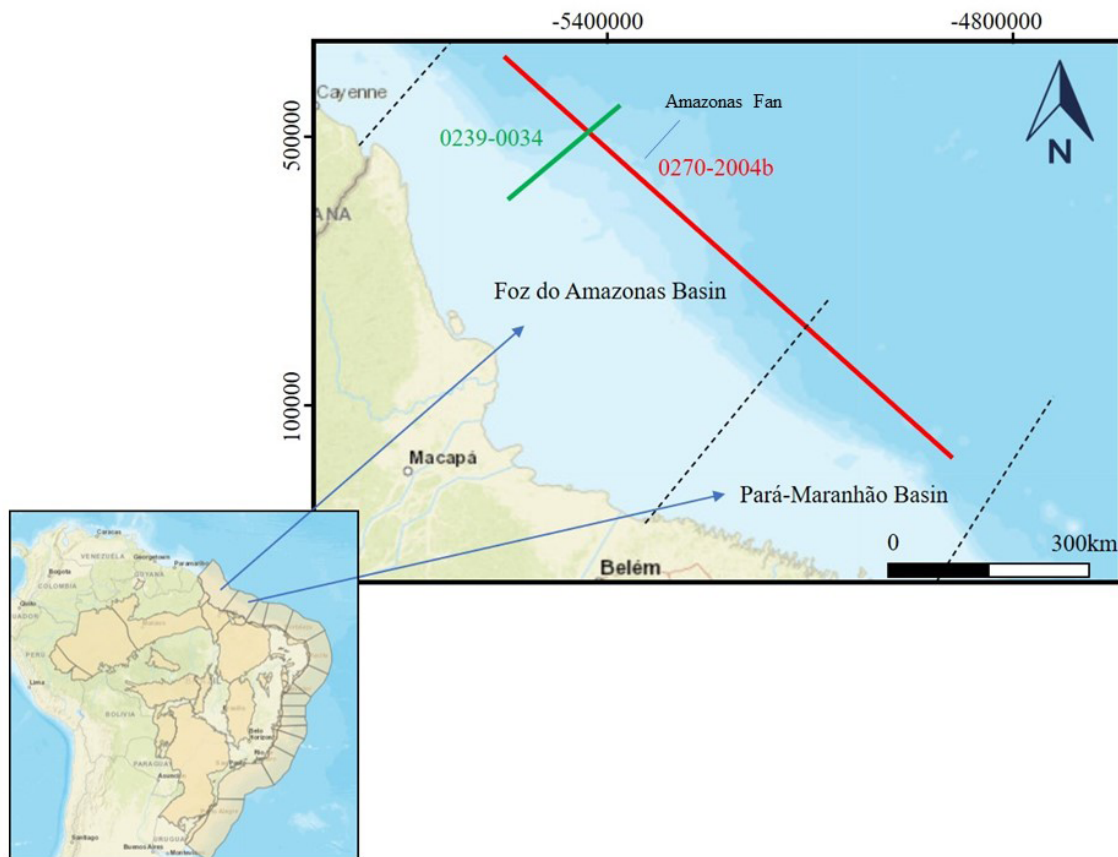


**Figure 1.** Location of the 2D seismic lines in the Amazon Deep Sea Fan, Foz do Amazonas Basin.

widely used in the exploration industry since it contributes to optimizing reservoir characterization. By interpreting in the frequency domain, additional information from seismic data can be extracted, such as thin-bed interference, geological discontinuities and detection of anomalies connected to the accumulation of hydrocarbons (Partyka *et al.* 1999).

Seismic attributes analyses have been used in different regions worldwide to investigate the existence of gas hydrates (Coren *et al.* 2001, Freire *et al.* 2011, Satyavani *et al.* 2008, Ojha and Sain 2009, Oliveira and Oliveira 2009, Oliveira *et al.* 2010, Aguiar *et al.* 2019), allowing the recognition of BSR and its continuity (Coren *et al.* 2001). Therefore, it can help to infer patterns linked to the allocation of gas hydrates and free gas below the GHSZ (Satyavani *et al.* 2008).

The main goal of the present study is to apply techniques to enhance BSR visualization, helping in the identification of gas hydrate occurrences in the Foz do Amazonas Basin. In our approach, we performed a comparison between seismic amplitudes of the seafloor and the BSR, in addition to the application of seismic attribute Envelope and spectral decomposition, which decomposed the seismic data into different frequency bands for each seismic section.

## Geologic setting

The Amazon Deep Sea Fan (Fig. 1) is the most prominent morphological feature of the Foz do Amazonas Basin, extending for about 700 km from the continental shelf break

to nearly 4,800 mbsl (Rimington *et al.* 2000, Araújo *et al.* 2009, Perovano *et al.* 2009). Its formation is associated to a high rate of siliciclastic sedimentation input to the Atlantic Ocean, since the middle Miocene, as a result of the uplift of the Andes Mountain Chain (Pasley *et al.* 2004, Figueiredo *et al.* 2007). The Amazon Fan deposition is related to the Andean Orogeny that caused the inversion of the Amazon River (Carvalho 2008), transforming the Amazon River into a major drainage system during the late Miocene (Rimington *et al.* 2000, Pasley *et al.* 2004). The fan was divided by Damuth and Kumar (1975) in three compartments according to changes in its gradient: upper (from shelf-break to -3,000 m isobath), middle (from -3,000 to -4,200 m), and lower (from -4,200 to -4,800 m). Cobbold *et al.* (2004) estimated that the fan has a thickness of approximately 10 km, with an average sedimentation rate of 1 m/ka.

The extreme sediment load drives the gravitational collapse of the fan, creating a proximal extensional domain with normal faults on the outer continental shelf and upper slope, and an outer compressional domain with thrust faults and folds, in the upper-fan (Reis *et al.* 2010, 2016). Extensive mass-transport deposits (MTD) prevails across the fan, interlayered with channel-levee systems, representing the Neogene stratigraphic succession (Araújo *et al.* 2009, Reis *et al.* 2010, 2016, Silva *et al.* 2016). Additionally, voluminous MTD complexes occur on the northwestern and southeastern flanks of the submarine fan. Several authors attribute MTD to gravitational landslides triggered by the dissociation of gas hydrates (Piper *et al.* 1997, Maslin *et al.* 2005, Araújo *et al.* 2009).

Ketzer *et al.* (2018) identified gas seeps and sampled gas hydrates on the Amazon Fan. About 60% of gas vents are located in the upper fan, along seafloor faults induced by undergoing gravitational collapse of the fan, while 40% are located in water depths of 650–715 m within the *feather* edge of the GHSZ (Ketzer *et al.* 2018).

## MATERIALS AND METHODS

From a regional 2D seismic dataset, we selected two seismic lines where prominent BSR were clearly observed cutting across deformed strata on the compressional domain within the upper-fan. The seismic sections identified as 0270-2004b and 0239-0034 are located in Figure 1 and presented in Figures 2 and 3,

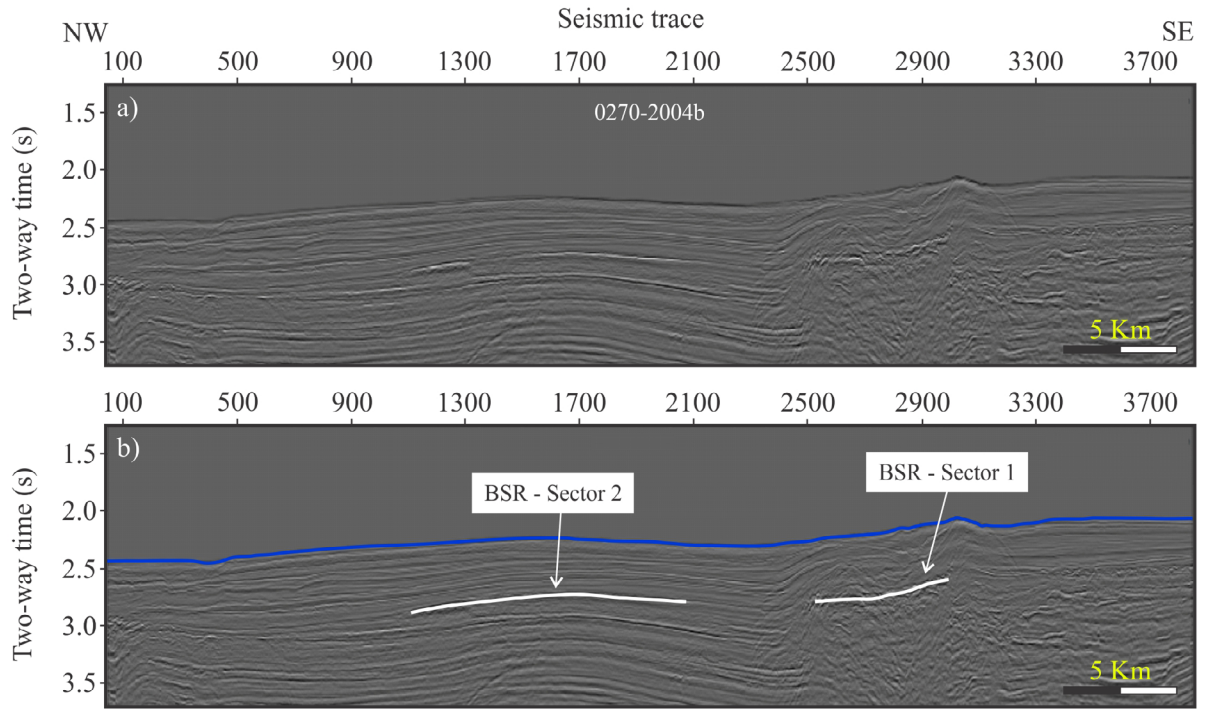


**Figure 2.** Non-interpreted (top) and interpreted (bottom) seismic line 0270-2004b displaying the two sectors of BSR (white). In sector 1, the BSR cuts across deformed strata of the Amazon Deep-Sea Fan compressional domain.

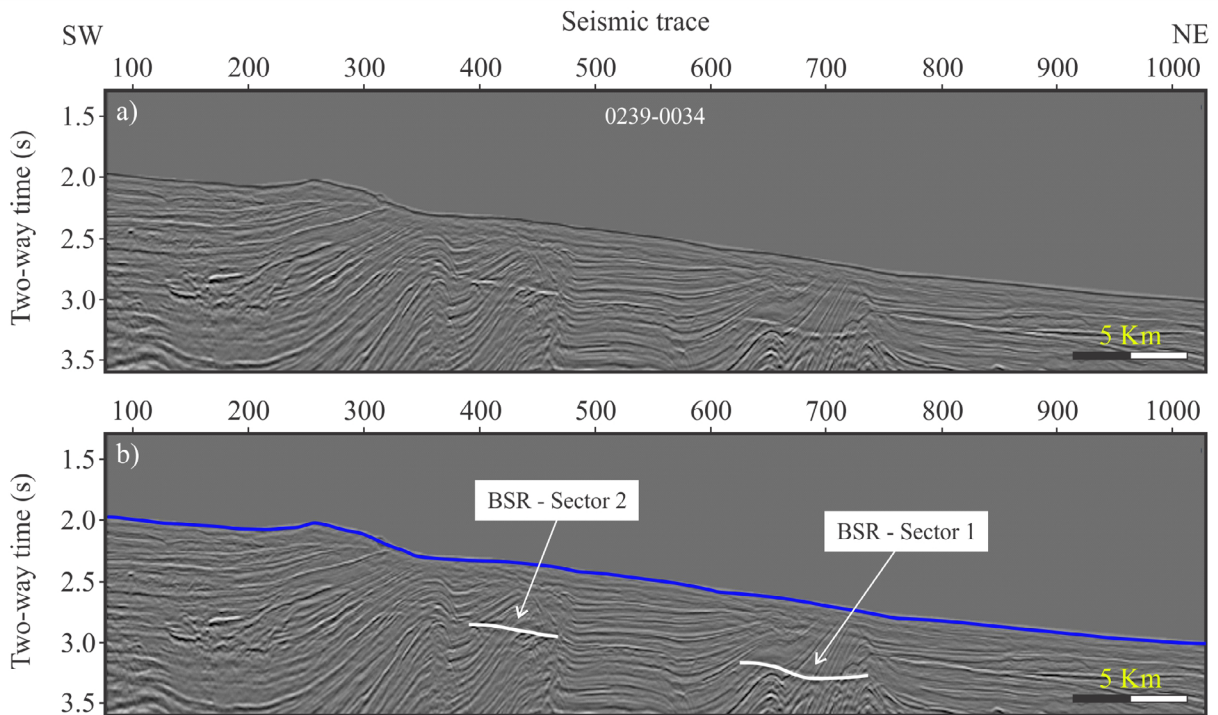


**Figure 3.** Non-interpreted (top) and interpreted (bottom) seismic line 0239-0034 displaying the two sectors of BSR (white), cutting across deformed strata of the Amazon Deep-Sea Fan compressional domain.



respectively. BSR occurrences are discontinuous and were divided into sectors one and two in both seismic sections, to facilitate interpretation (Figs. 2 and 3).

After picking the seafloor and BSR, we automatically extracted the correspondent amplitude values for every seismic trace, using the “extract value” tool from the Petrel® software, by Schlumberger. Amplitude values for every trace were plotted for subsequent analysis.

Different seismic attributes were applied to emphasize the BSR visualization and to suggest the BGHSZ. The envelope was the seismic attribute that most enhanced the reflector. The generalized spectral decomposition attribute (GSD) provides the contribution of individual frequencies to the makeup of the input seismic signal and resulted in the selection of three influential frequency bands: 20 Hz, 30 Hz, and 40 Hz. After GSD, a -90° phase rotation was applied for each section decomposed in the frequency bands mentioned. Subsequently, we calculated the envelope attribute for each band to highlight the lateral continuity of the anomalies. When performing this flow to calculate the attribute, we are inferring layer properties instead of interfaces.

The workflow to identify and analyze BSR in seismic sections in the Foz do Amazonas Basin is summarized in Figure 4.

### RESULTS AND DISCUSSION

Figures 2 and 3 show, respectively, seismic sections 0270-2004b and 0239-0034 with the interpretation of the seafloor (blue) and BSR sectors (white) that were identified by reflections of negative amplitudes parallel to the seafloor.

As Majumdar *et al.* (2016) declared, the interpretation of a BSR on seismic data might be subjective, such that presents inherent uncertainty. The recognition of BSR in deformed substrate is easily demonstrated when it cuts strata reflections that are not parallel to the seafloor (Holbrook *et al.* 2002, Freire *et al.* 2011, Aguiar *et al.* 2019). However, when BSR occurrences are located in non-deformed strata, where reflectors are parallel to the seabed, its recognition is not always trivial. Therefore, additional approaches for identifying BSR truly associated with gas hydrates are greatly welcome.

### Seismic amplitude comparisons

The gas hydrate stability zone (GHSZ) corresponds to the vertical interval starting at the seafloor and extending to the base of this zone, in which pressure and temperature conditions are appropriate for gas hydrate stability (Majumdar *et al.* 2016). As stated by Kvenvolden (1993), the reflector that matches the BGHSZ is characterized by a polarity reverse to the seafloor reflector. In theory, the amplitudes of BSR are higher due to the large contrast of acoustic impedance caused by the presence of the free gas below and hydrates above (Dillon *et al.* 1996). Therefore, most of the reflection amplitude of BSR is caused by the underlying free gas (Haacke *et al.* 2007).

To verify the position of the BSR and presume the occurrence of gas hydrates related to these reflectors, we compared the seismic amplitudes for the two sectors of BSR in sections 0270-2004b and 0239-003. Seafloor and BSR amplitude plots, for data picked automatically in sectors 1 and 2, along both seismic sections are shown in Figures 5 and 6. The purpose of extracting seismic amplitudes automatically is to investigate

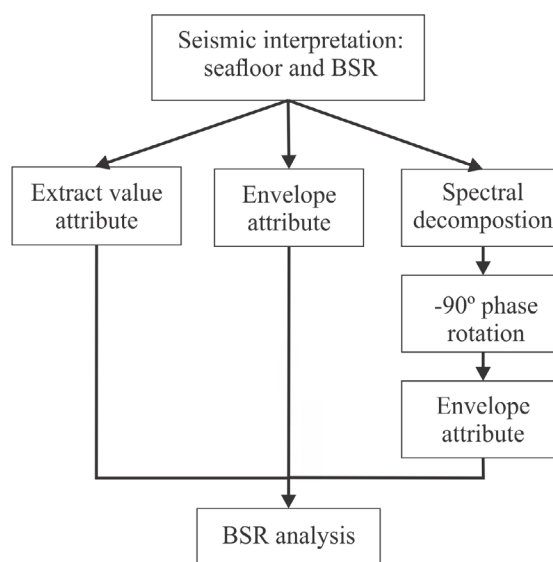


Figure 4. Proposed workflow applied for the analysis of BSR.

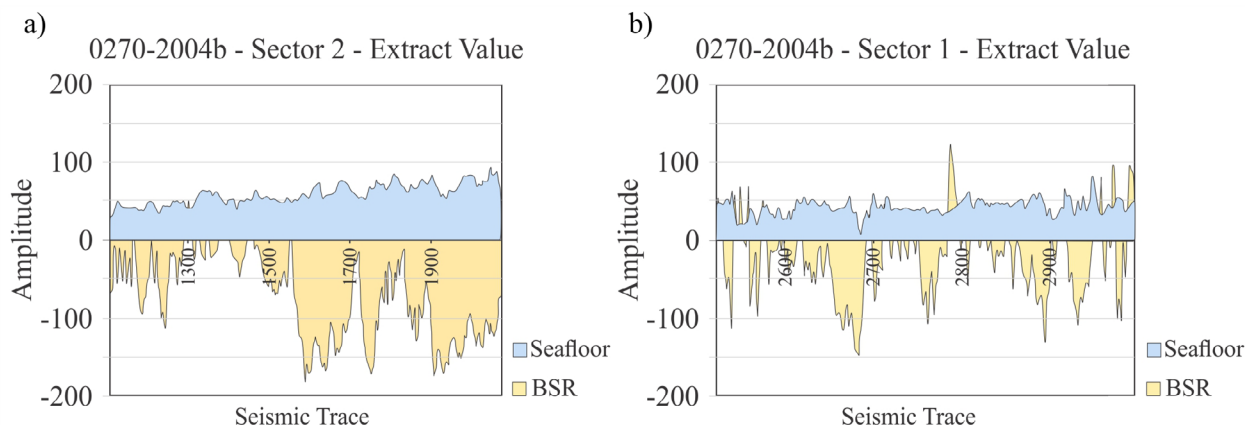
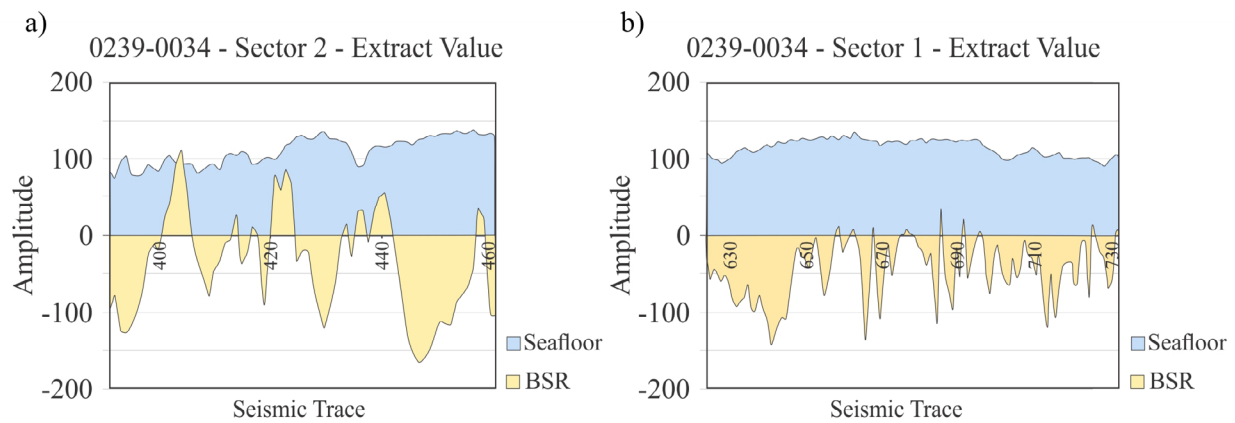


Figure 5. Seismic amplitude plots of section 0270-2004b after extracting the amplitude values for the seafloor (blue) and the BSR (orange) along sectors 1 and 2. BSR values are mostly negative and large; however, there are portions with positive values, implying BSR discontinuity.



**Figure 6.** Seismic amplitude plots of section 0239-0034 after extracting the amplitude values for the seafloor (blue) and the BSR (orange) along sectors 1 and 2. These graphs were considerably smooth but intervals of positive values, especially on sector 2, suggests a lateral discontinuity of the BSR.

how this approach supports recognizing BSR. It might be spontaneous to consider that extracting values automatically through an interpreted horizon is more accurate than a manual extraction, since the software selects wiggles associated to the same seismic event. In addition, amplitude values are extracted for every seismic trace, which increases their reliability. Another advantage of using the automatic approach is the fact that this procedure consumes considerably less time than the manual pick, which could be impractical in cases with large volumes of data.

The graphics displayed in Figures 5 and 6 have the reverse amplitudes between the seafloor (positive) and the assumed BSR (negative), as expected. There are portions where values from BSR amplitudes are extremely high, which helps the recognition of this reflector. We can observe that some intervals register positive amplitudes in reflectors initially interpreted as BSR, especially for sector 2 in line 0239-0034 (Fig. 6A), which is not possible, by definition. This means that the BSR is discontinuous, probably due to a low contrast ratio between the hydrate zone, above, and the free gas zone, below, which suggests a lateral discontinuity of the BSR in these intervals.

As stated by Holbrook *et al.* (2002), BSR amplitude is susceptible to gas concentrations placed below the GHSZ. Besides, Dillon *et al.* (1996) suggest that BSR is presented discontinuous at higher frequencies, which would form a sequence of marked reflections parallel to the seafloor, but laterally discontinuous. Therefore, this justifies the small intervals where the absolute values of seismic amplitudes among the seafloor and the BSR are divergent. The related contrast in impedance between gas hydrates located above the BGHSZ, and of free gas under it, are not the same and causes the intensity variation of the BSR amplitude (Freire *et al.* 2011). Hence, the BSR will have higher amplitude values the greater the impedance contrast (Aguiar *et al.* 2019).

### Application of the envelope attribute

The envelope attribute (instantaneous amplitude) is a suitable discriminator for stratigraphic and lithological changes in accumulations of gas and oil in reservoirs (Chen and Sidney

1997, Taner 2001), being used here as indicative of free gas confined underneath the BSR. Figures 7 and 8 show, respectively, sections 0270-2004b and 0239-0034 with the envelope attribute and the interpreted BSR (bottom).

The envelope attribute reinforces the strongest reflections and suggests the continuity of the BSR extending further laterally. However, the application of this attribute only accentuated the portions where the interpreted BSR was already well marked in the amplitude sections, which advocates for the importance of using other indirect tools combined to best highlight its visualization. This probably results from the concentrations of gas hydrates within the hydrate stability zone and of free gas below this zone, which causes the strength of the reflector to modify locally (Freire *et al.* 2011).

### Application of the spectral decomposition

Initially a study of the frequency spectrum was performed to analyze the best frequency bands that can represent gas hydrates reservoirs. Figure 9 shows two graphics containing the frequency spectra from each seismic section.

The seismic sections were decomposed in frequency bands only at intervals that include the BSR. For the seismic line 0239-0034, the interval selected was between 1.9/3.4 seconds, and 2.0/3.1 seconds for the seismic section 0270-2004b. From the analysis of the frequency spectrum plots displayed above, three frequency bands centered in 20Hz, 30Hz, and 40Hz were chosen. Higher frequency bands were also tested but did not present relevant results. As frequency band increases, the BSR is enhanced and its discontinuity becomes more evident (Figs. 10A to 13A). The same seismic sections decomposed in different frequency bands are presented after applying the envelope attribute and a -90 degrees phase rotation (Figs. 10B to 13B). The results show the improvement in the visualization of BSRs and their lateral continuity in areas where they were not previously seen.

Gas hydrates reservoirs are generated only when there is an amount of water and gas to create them, and in a suitable pressure and temperature (Kvenvolden 1998, Sloan Jr. 2003). As stated by Haacke *et al.* (2007), a known methane hydrate recycling mechanism generates gas from the dissociation of

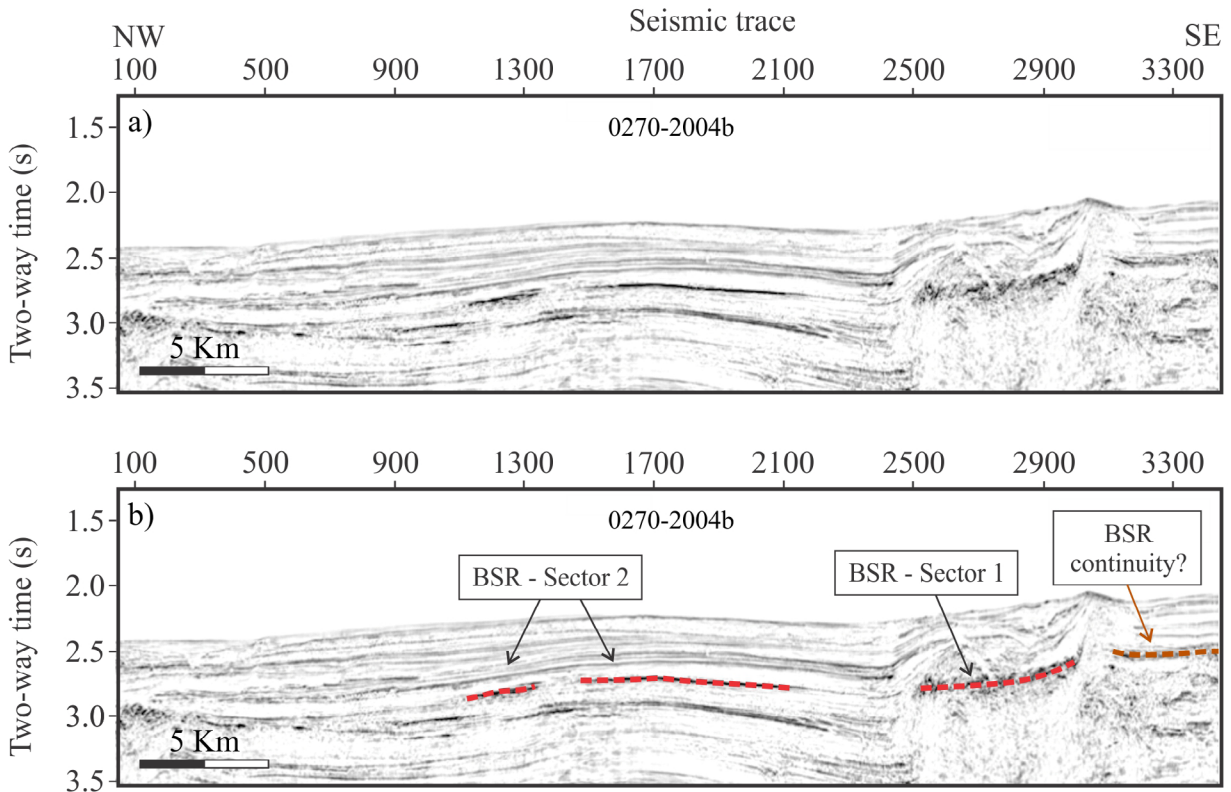


**Figure 7.** Seismic section 0270-2004b with the envelope attribute, suggesting the BSR continuity to the southeast of sector 1.

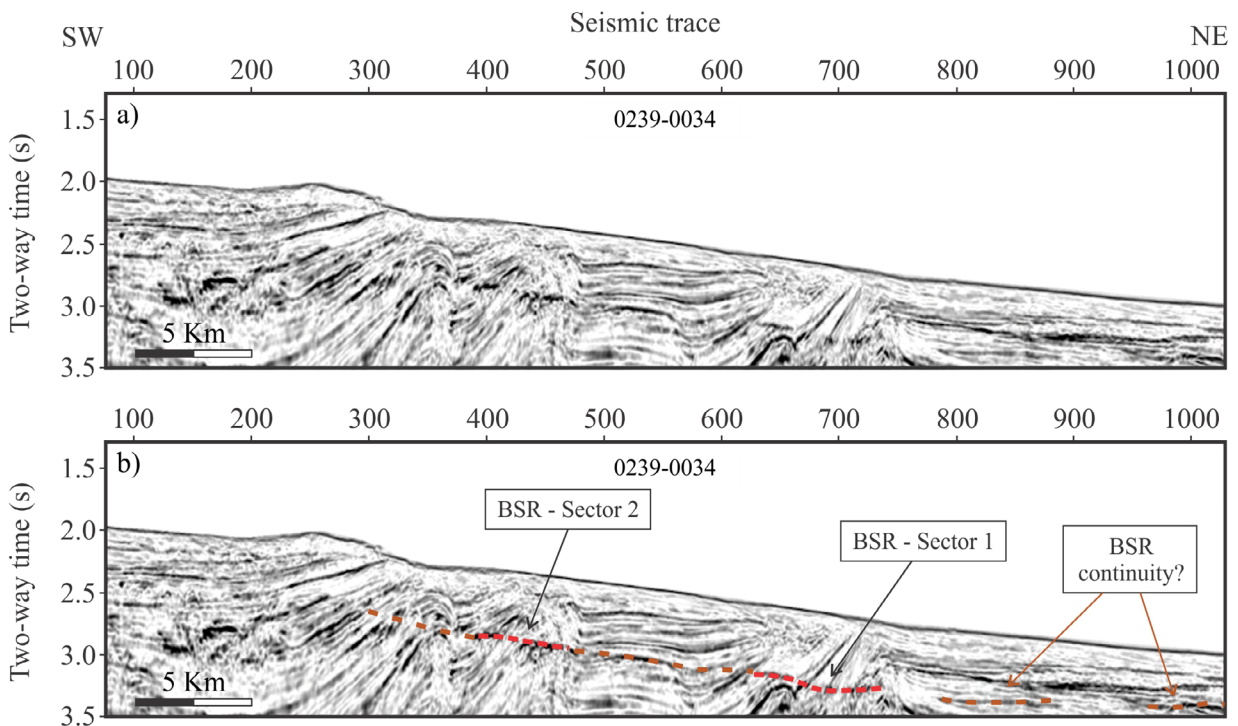


**Figure 8.** Seismic section 0239-0034 with the envelope attribute, suggesting the continuity of the BSRs in between sectors 1 and 2 and further to the SW and NE.

gas hydrate. Thus, the base of the GHSZ moves upward relative to hydrate-bearing zone. If there is still gas but no longer enough water to combine and to produce gas hydrates, then the hydrates might work as a seal, forming a barrier that retains gas within the gas hydrate stability zone. This could be

a justification for portions that were intensely enhanced by using spectral decomposition with envelope attribute, such as observed in Figure 11.

The utilization of the spectral decomposition and envelope attributes aided enriched interpretation, especially due to their



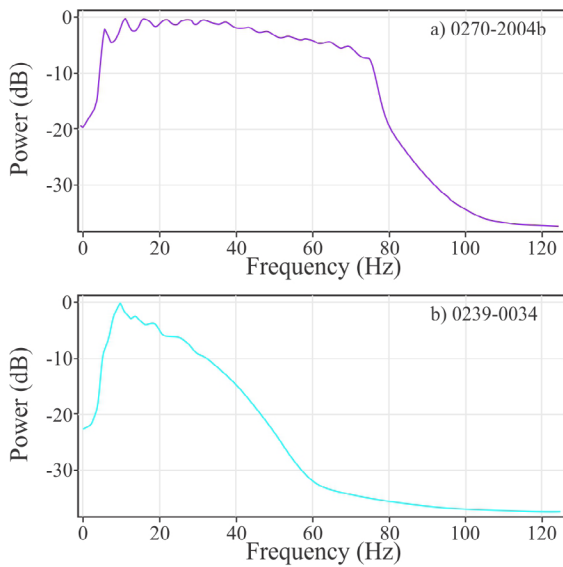


**Figure 9.** Frequency spectra for seismic sections (A) 0270-2004b, and (B) 0239-0034.

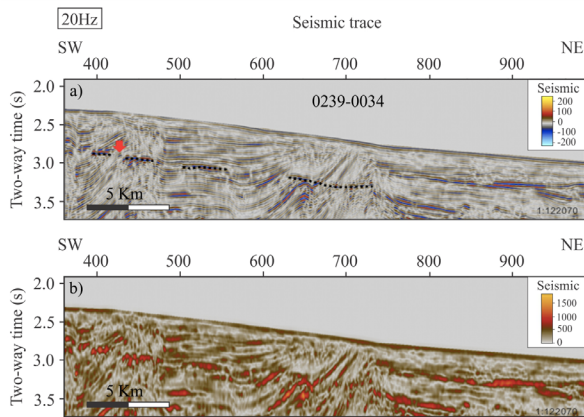


**Figure 10.** Seismic section 0239-0034 with the 20 Hz decomposed frequency band (top) and with the  $-90^\circ$  phase rotation and the envelope attribute (bottom). The sectors interpreted as BSR are displayed in black. The red arrow indicates a discontinuity of BSR that became more evident after applying spectral decomposition.

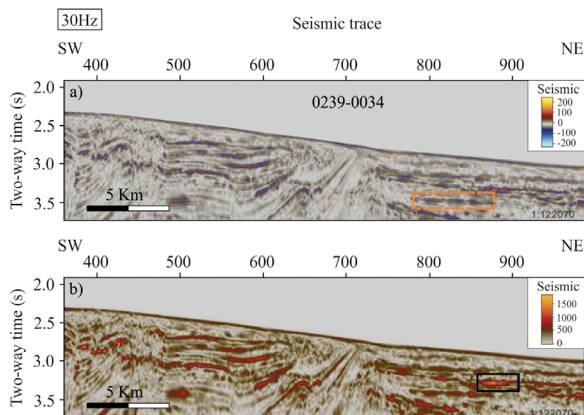


**Figure 11.** Seismic section 0239-0034 with the 30 Hz decomposed frequency band (top) and with the  $-90^\circ$  phase rotation and the envelope attribute (bottom). The black box (bottom) can indicate a zone within the GHSZ where the saturation of free gas is higher. The orange box (top) reinforces the interpretation of BSR continuity, also observed with the envelope attribute (Fig. 8).

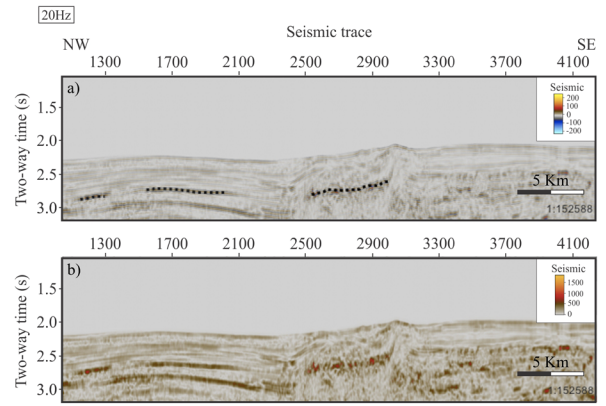


**Figure 12.** Seismic section 0270-2004b with the 20 Hz decomposed frequency band (top) and with the  $-90^\circ$  phase rotation and the envelope attribute (bottom). BSR is displayed in black. Lateral discontinuity of BSR can be noticed in the two sectors.

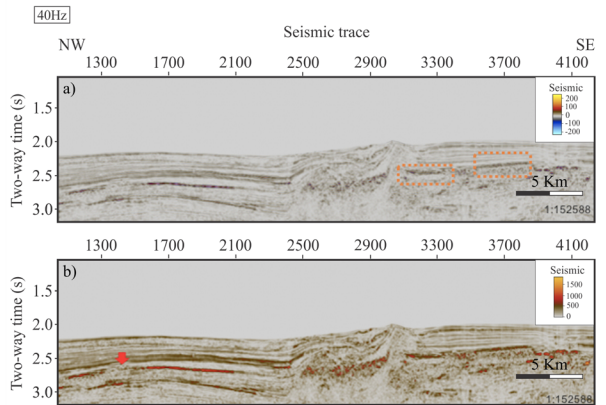


**Figure 13.** Seismic section 0270-2004b with the 40 Hz decomposed frequency band (top) and with the  $-90^\circ$  phase rotation and the envelope attribute (bottom). The red arrow (bottom) shows the lateral discontinuity of BSR. The orange boxes (top) highlight possible BSR continuity, also noticed with the envelope attribute (Fig. 7).

contribution to identifying portions where BSR is laterally discontinuous and portions where new possibilities on BSR continuity are enhanced. They also highlighted the free gas trapped underneath the BSR and enhanced portions where methane hydrates probably work as seals, such as observed for seismic section 0239-0034. Although frequency bands 30 Hz–40 Hz showed fine results, a regular pattern was not observed in the frequency decomposition to help improving BSR visualization.

The following approaches corroborate the findings of this study, indicating the wealth of information that can be derived from the seismic data in the recognition of gas hydrates reservoirs, justifying dedicated seismic surveys to study specifically shallow gas hydrates.

Gas hydrates reservoirs can be present even in areas where BSR are not noted (Satyavani *et al.* 2008), which advocates for the worth of studying indirect methodologies to determine the occurrence of hydrates. Consequently, employing seismic attributes, such as the envelope attribute (Satyavani *et al.* 2008, Joshi *et al.* 2017) as an instrument for interpreting BSR in seismic is applicable for a better understanding of its distribution.

Coren *et al.* (2001) indicated a multi-attribute evaluation for improving the characterization of BSR, whereas Satyavani *et al.* (2008) propose the utilization of amplitude *versus* offset (AVO) to obtain data on free gas occurrence under the BSR. Oliveira and Oliveira (2009) and Oliveira *et al.* (2010) used spectral decomposition to identify seismic features related to methane hydrates in the Pelotas Basin, such as low-frequency blackout zone, blanking and gas flow, and therefore to assume distribution of gas hydrate and also free gas.

By comparing the results of this manuscript with the ones obtained by Aguiar *et al.* (2019), we highlight some considerations: results show similarities in terms of the reversal of polarities between the seafloor and the interpreted BSR, and also when the BSR is enhanced through the application of the seismic attribute envelope. The key differences are related to the application of spectral decomposition. This technique not only allowed enhancing this anomalous reflector but also improved the visualization of BSR and their lateral continuity, including areas that were not identified before.

## CONCLUSIONS

Different approaches for the identification of BSR were tested, including: identification of negative amplitude reflections, the automatic confrontation of seismic amplitudes, and

analysis of envelope and spectral decomposition attributes. In conjunction, these approaches validated the position of the BSR in the seismic sections which revealed to be a valuable technique for understanding gas hydrate distribution in the Foz do Amazonas Basin, and can be used in other similar sites. The reversal of signal polarities among the seafloor (positive) and the BSR (negative) can be a preliminary indicator of a correct recognition of BSR, even though it is not constant. The envelope attribute was capable to emphasize the visualization of BSR for the different sections, especially within frequency bands 30Hz–40Hz. The attribute obtained from the spectral decomposition, -90° phase rotation and envelope helped to identify portions where BSR is laterally discontinuous, additionally highlighting portions where gas hydrates work as seals, retaining free gas within the GHSZ.

## ACKNOWLEDGMENTS

The authors are grateful to the National Agency of Petroleum for the authorization to work on the seismic data of the Foz do Amazonas Basin. They are also grateful to Schlumberger, for providing the Petrel Software. The first author thanks the National Council for Scientific and Technological Development and the Coordination for Academic Level Improvement for the financial support.

## ARTICLE INFORMATION

Manuscript ID: 20200075. Received on: 07/21/2020. Approved on: 11/17/2020.

L.A. wrote the first draft of the manuscript and prepared all figures; A.F. provided advisorship regarding gas hydrates, regional geology, and seismic interpretation; improved the manuscript through corrections and suggestions; C.S. provided advisorship regarding gas hydrates, regional geology, and seismic interpretation; improved the manuscript through corrections and suggestions; W.L. provided advisorship regarding seismic interpretation and seismic attributes; improved the manuscript through corrections and suggestions.

Competing interests: The authors declare no competing interests.

## REFERENCES

- Aguiar L.F., Freire A.F.M., Santos L.A., Dominguez A.C.F., Neves E.H.P., Silva C.G., Santos M.A.C. 2019. Analysis of seismic attributes to recognize bottom simulating reflectors in the Foz do Amazonas basin, Northern Brazil. *Revista Brasileira de Geofísica*, **37**(1):43-53. <https://doi.org/10.22564/rbgf.v37i1.1988>
- Araújo E.F.S., Silva C.G., Reis A.T., Perovano R., Gorini C., Vendeville B.C., Albuquerque N.C. 2009. Movimentos de Massa Multiescala na Bacia da Foz do Amazonas - Margem Equatorial Brasileira. *Revista Brasileira de Geofísica*, **27**(3):485-508. <https://doi.org/10.1590/S0102-261X2009000300013>
- Berryman J., Kearns H., Rodriguez K. 2015. Foz do Amazonas Basin- A case for oil generation from geothermal gradient modelling. *First Break*, **33**(11):91-95.
- Brandão J.A.S.L., Feijó F.J. 1994. Bacia da Foz do Amazonas. *Boletim de Geociências da Petrobras*, **8**(1):91-99.
- Carvalho G.C.R.D. 2008. *Interpretação sísmica e modelagem física do cone do Amazonas, Bacia da Foz do Amazonas, margem equatorial brasileira*. Master's dissertation. Ouro Preto: Departamento de Geologia, Escola de Minas, Universidade Federal de Ouro Preto, 119 p.
- Chen Q., Sidney S. 1997. Seismic attribute technology for reservoir forecasting and monitoring. *The Leading Edge*, **16**(5):445-448. <https://doi.org/10.1190/1.1437657>
- Cobbold P.R., Mourgues R., Boyd K. 2004. Mechanism of thin-skinned detachment in the Amazon Fan: assessing the importance of fluid overpressure and hydrocarbon generation. *Marine and Petroleum Geology*, **21**(8):1013-1025. <https://doi.org/10.1016/j.marpetgeo.2004.05.003>
- Coren F., Volpi V., Tinivella U. 2001. Gas hydrate physical properties imaging by multi-attribute analysis - Blake Ridge BSR case history. *Marine Geology*, **178**(1-4):197-210. [https://doi.org/10.1016/S0025-3227\(01\)00156-6](https://doi.org/10.1016/S0025-3227(01)00156-6)
- Damuth J.E., Kumar N. 1975. Amazon Cone: Morphology, Sediments, Age, and Growth Pattern. *Bulletin of the Geological Society of America*, **86**(6):863-878. [https://doi.org/10.1130/0016-7606\(1975\)86<863:ACMSAA>2.0.CO;2](https://doi.org/10.1130/0016-7606(1975)86<863:ACMSAA>2.0.CO;2)
- Demirbas A. 2010. Methane hydrates as potential energy resource: Part 1 - Importance, resource and recovery facilities. *Energy Conversion and Management*, **51**(7):1547-1561. <https://doi.org/10.1016/j.enconman.2010.02.013>
- Di Profio P., Canale V., D'Alessandro N., Germani R., Di Crescenzo A., Fontana A. 2017. Separation of CO<sub>2</sub> and CH<sub>4</sub> from biogas by formation of clathrate hydrates: Importance of the driving force and kinetic promoters. *ACS Sustainable Chemistry and Engineering*, **5**(2):1990-1997. <https://doi.org/10.1021/acsschemeng.6b02832>
- Dillon W.P., Hutchinson D.R., Drury R.M. 1996. Seismic Reflection Profiles on the Blake Ridge near sites 994, 995, and 997. *Proceedings of the Ocean Drilling Program*, **164**:47-56. <https://doi.org/10.2973/odp.proc.ir.164.104.1996>
- Figueiredo J.J.P., Zalán P.V., Soares E.F. 2007. Bacia da foz do Amazonas. *Boletim de Geociências da Petrobras*, **15**(2):299-309.



- Freire A.F.M., Matsumoto R., Santos L.A. 2011. Structural-stratigraphic control on the Umitaka Spur gas hydrates of Joetsu Basin in the eastern margin of Japan Sea. *Marine and Petroleum Geology*, **28**(10):1967-1978. <https://doi.org/10.1016/j.marpetgeo.2010.10.004>
- Ginsburg G.D., Soloviev V.A. 1997. Methane migration within submarine gas-hydrate stability zone under deep-water conditions. *Marine Geology*, **137**(1-2):49-57. [https://doi.org/10.1016/S0025-3227\(96\)00078-3](https://doi.org/10.1016/S0025-3227(96)00078-3)
- Haacke R.R., Westbrook G.K., Hyndman R.D. 2007. Gas hydrate, fluid flow and free gas: Formation of the bottom-simulating reflector. *Earth and Planetary Science Letters*, **261**(3-4):407-420. <https://doi.org/10.1016/j.epsl.2007.07.008>
- Holbrook W.S., Hoscinks W.T., Wood R.A., Stephen G.D., Lizarralde D. 1996. Methane hydrate and free-gas on the Blake Ridge from vertical seismic profiling. *Science*, **273**(5283):1840-1843. <https://doi.org/10.1126/science.273.5283.1840>
- Holbrook W.S., Gorman A.R., Hornbach M., Hackwith K.L., Nealon J., Lizarralde D., Pecher I.A. 2002. Seismic detection of marine methane hydrate. *The Leading Edge*, **21**(7):686-689. <https://doi.org/10.1190/1.1497325>
- Hyndman R.D., Spence G.D. 1992. A seismic study of methane hydrate marine bottom simulating reflectors. *Journal of Geophysical Research*, **97**(B5):6683-6698. <https://doi.org/10.1029/92JB00234>
- Joshi A.K., Pandey L., Sain K. 2017. Identification of BSR and estimation of gas hydrate from well-log data at NGHP-01-04A and 11A in the Krishna-Godavari Basin, Eastern Indian Margin. *SEG Technical Program Expanded Abstracts*, 3483-3487. <https://doi.org/10.1190/segam2017-17791181.1>
- Ketzer J.M., Augustin A., Rodrigues L.F., Oliveira R., Praeg D., Pivel M.A.G., Reis A.T., Silva C., Leonel B. 2018. Gas seeps and gas hydrates in the Amazon deep-sea fan. *Geo-Marine Letters*, **38**(5):429-438. <https://doi.org/10.1007/s00367-018-0546-6>
- Kvenvolden K.A. 1993. Gas hydrates-Geological Perspective and Global Change. *Reviews of Geophysics*, **31**(2):173-187. <https://doi.org/10.1029/93RG00268>
- Kvenvolden K.A. 1998. A primer on the geological occurrence of gas hydrate. *Geological Society Special Publication*, **137**(1):9-30. <https://doi.org/10.1144/GSL.SP.1998.137.01.02>
- Majumdar U., Cook A.E., Shedd W., Frye M. 2016. The connection between natural gas hydrate and bottom-simulating reflectors. *Geophysical Research Letters*, **43**(13):7044-7051. <https://doi.org/10.1002/2016GL069443>
- Manley L., Flood R.D. 1988. Cyclic Sediment Deposition Within Amazon Deep-Sea Fan. *The American Association of Petroleum Geologists Bulletin*, **72**(8):912-925.
- Maslin M., Vilela C., Mikkelsen N., Grootes P. 2005. Causes of catastrophic sediment failures of the Amazon Fan. *Quaternary Science Reviews*, **24**(20-21):2180-2193. <https://doi.org/10.1016/j.quascirev.2005.01.016>
- Ojha M., Sain K. 2009. Seismic attributes for identifying gas-hydrates and free-gas zones: Application to the Makran accretionary prism. *Episodes*, **32**(4):264-270. <https://doi.org/10.18814/epiiugs/2009/v32i4/003>
- Oliveira O.M.V., Oliveira S.A.M. 2009. Aplicação Da decomposição espectral de dados sísmicos no estudo das acumulações de hidratos de gás da bacia de Pelotas. In: International Congress of the Brazilian Geophysical Society, 11., 2009. *Proceedings...* [https://doi.org/10.3997/2214-4609-pdb.195.1438\\_evt\\_6year\\_2009](https://doi.org/10.3997/2214-4609-pdb.195.1438_evt_6year_2009)
- Oliveira S., Vilhena O., Costa E. 2010. Time-frequency spectral signature of Pelotas Basin deep water gas hydrates system. *Marine Geophysical Research*, **31**(1):89-97. <https://doi.org/10.1007/s11001-010-9085-x>
- Partyka G., Gridley J., Lopez J. 1999. Interpretational applications of spectral decomposition in reservoir characterization. *The Leading Edge*, **18**(3):353. <https://doi.org/10.1190/1.1438295>
- Pasley M.A., Shepherd D.B., Pocknall D.T., Boyd K.P., Andrade V., Figueiredo J.P. 2004. Sequence stratigraphy and basin evolution of the Foz do Amazonas Basin, Brazil. In: AAPG International Conference & Exhibition, 2004. *Proceedings...* Cancun, Boulder: American Association of Petroleum Geologists, p. 12.
- Perovano R., Reis A.T., Silva C.G., Vendeville B.C., Gorini C., Oliveira V., Araújo E.F.S. 2009. O Processo de colapso gravitacional da seção marinha da Bacia da Foz do Amazonas – Margem equatorial brasileira. *Revista Brasileira de Geofísica*, **27**(3):459-484. <http://doi.org/10.1590/S0102-261X2009000300012>
- Piper D.J.W., Pirmez C., Manley P.L., Long D., Flood R.D., Normark W.R., Showers W. 1997. Mass-transport deposits of the Amazon Fan. In: *Proceedings of the Ocean Drilling Program, Scientific Results*, **155**:109-146.
- Reis A.T., Araújo E., Silva C.G., Cruz A.M., Gorini C., Droz L., Migeon S., Perovano R., King I., Bache F. 2016. Effects of a regional décollement level for gravity tectonics on late Neogene to recent large-scale slope instabilities in the Foz do Amazonas Basin, Brazil. *Marine and Petroleum Geology*, **75**:29-52. <https://doi.org/10.1016/j.marpetgeo.2016.04.011>
- Reis A.T., Perovano R., Silva C.G., Vendeville B.C., Araújo E., Gorini C., Oliveira V. 2010. Two-scale gravitational collapse in the Amazon Fan: a coupled system of gravity tectonics and mass-transport processes. *Journal of the Geological Society*, **167**(3):593-604. <http://doi.org/10.1144/0016-76492009-035>
- Rimington N., Cramp A., Morton A. 2000. Amazon Fan sands: implications for provenance. *Marine and Petroleum Geology*, **17**(2):267-284. [https://doi.org/10.1016/S0264-8172\(98\)00080-4](https://doi.org/10.1016/S0264-8172(98)00080-4)
- Sad A.R.E., Silveira D.P., Machado D.A.P., Silva S.R.P., Maciel R.R. 1998. Marine gas hydrates evidence along the Brazilian coast. In: AAPG International Conference and Exhibition, 1998. *Proceedings...*
- Satyavani N., Sain K., Lall M., Kumar B.J.P. 2008. Seismic attribute study for gas hydrates in the Andaman Offshore India. *Marine Geophysical Research*, **29**(3):167-175. <https://doi.org/10.1007/s11001-008-9053-x>
- Silva C.G., Reis A.T., Perovano R.J., Gorini M.A., Santos M.V.M., Jeck I.K., Tavares A.A.A., Gorini C. 2016. Multiple megaslide complexes and their significance for the Miocene stratigraphic evolution of the offshore Amazon Basin. In: Lamarche G., Mountjoy J., Bull S., Hubble T., Krastel S., Lane E., Micallef A., Moscardelli L., Mueller C., Pecher I., Woelz S. (eds.). *Submarine mass movements and their consequences*. Advances in Natural and Technological Hazards Research 41, p. 49-60. Suíça: Springer. [https://doi.org/10.1007/978-3-319-20979-1\\_5](https://doi.org/10.1007/978-3-319-20979-1_5)
- Sloan Jr. E.D. (2003). Fundamental principles and applications of natural gas hydrates. *Nature*, **426**(6964):353-359. <https://doi.org/10.1038/nature02135>
- Tanaka M.D., Silva C.G., Clennell M.B. 2003. Gas hydrates on the Amazon Submarine Fan, Foz do Amazonas Basin, Brazil. In: AAPG Annual Meeting, 2003. *AAPG Search and Discovery*. Salt Lake City.
- Taner M.T. 2001. Seismic Attributes. *CSEG Recorder*, **26**(7). Available at: <https://csegrecorder.com/articles/view/seismic-attributes>. Accessed on: Dec 12, 2019.
- Taner M.T., Koehler F., Sheriff R.E. 1979. Complex Seismic Trace Analysis. *Geophysics*, **44**(6):1041-1063. <https://doi.org/10.1190/1.1440994>
- Taner T., Schuelke J.S., O'Doherty R., Baysal E. 1994. Seismic attributes revisited. *SEG Technical Program Expanded Abstracts*, 1104-1106. <https://doi.org/10.1190/1.1822709>